Simulation and Design of Interline Power Flow Controller System

S.SANKAR
Faculty in Department of EEE, SCSVMV University, Kanchipuram, Tamil Nadu, India.
shankar_submanian@yahoo.co.in

Abstract: *To improve the power quality in distribution systems, Interline Power Flow controller (IPFC) was developed in this paper, this controller has been demonstrated to be successfully. Here the IPFC performance is to consider the DC-link voltage that represents in both two cases a real measure of the actual operating condition and of the interactions between the inverters and to modify the control inputs respectively. The flows of real and reactive powers were studied by using the circuit models developed for the IPFC system. The IPFC system is simulated using PSPICE and the simulation results are presented. The simulation results agree with the theoretical results*

Key words: *IPFC, POWER FLOW, FACTS, PSPICE.*

1. Introduction

In its general form the IPFC employs a number of dc/ac inverters each providing series compensation for a different line. An elementary configuration of IPFC consists of two dc/ac inverters connected in series with the transmission line and linked together at their DC terminals, as illustrated in Fig. 1. With this scheme any inverter can be controlled to supply real power to the common DC-link from its own transmission line. Naturally, one of the inverters, compensating overloaded lines or lines with a heavy burden of reactive power flow, can be equipped with full two-dimensional, reactive and real power control capability. Evidently, it is fundamental to maintenance in this arrangement the overall power balance at the common DC-link by appropriate control action.

The arrangement shown in Fig.1 can be functionally represented as in Fig. 2, where two synchronous voltage sources, with phasors $\overline{V}_{dq1}$ and $\overline{V}_{dq2}$, in series with the transmission lines 1 and 2, represent the two dc/ac series inverters (indicated in the following as SeV1 and SeV2, respectively). Transmission line 1, represented by reactance X_{l1}, has a sending-end bus with voltage phasor $\overline{V}_{s1}$ and a receiving-end bus with voltage phasor $\overline{V}_{r1}$. The sending-end voltage phasor of line 2, represented by reactance X_{l2}, is $\overline{V}_{s2}$ and the receiving voltage phasor is $\overline{V}_{r2}$.

For clarity, all the sending-end and receiving-end voltages are assumed to be constant with fixed amplitudes, $V_{s1}=V_{r1}=V_{s2}=V_{r2}$, and with fixed angles resulting in identical transmission angles, $\delta_1=\delta_2$ for the two transmission systems.

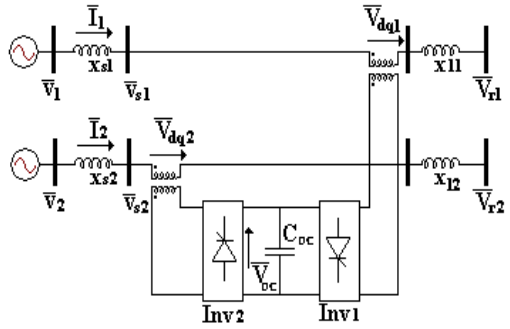

Fig. 1. Two inverters IPFC configuration

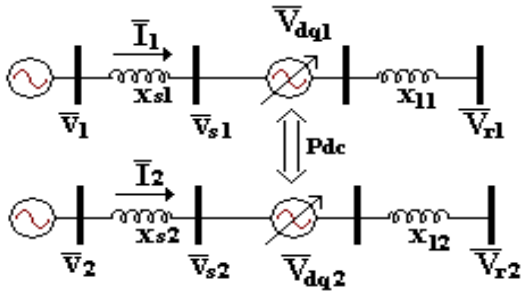

Fig. 2. Two inverters IPFC functional scheme

2. Mathematical Designing

In order to establish the transmission relationships between the two systems, system1 is arbitrarily selected to be the "prime" system for which free controllability of both real and reactive line power flow is stipulated. A phasor diagram of system 1, defining the relationship between $\overline{V}_{s1}$, $\overline{V}_{r1}$, $\overline{V}_{xl1}$ and the inserted voltage phasor $\overline{V}_{dq1}$ with controllable magnitude ($0\le V_{dq1}\le V_{dq1max}$) and angle ($0\le\beta_1\le360°$), is shown in Fig. 3.

The inserted voltage phasor $\overline{V}_{dq1}$ is added to the

fixed sending-end voltage phasor $\bar{V}_{s1}$ to produce the effective sending-end voltage $\bar{V}_{s1eff} = \bar{V}_{s1} + \bar{V}_{dq1}$. The difference $\bar{V}_{s1eff}$ - $\bar{V}_{r1}$, provides the compensated voltage phasor, $\bar{V}_{xl1}$, across X_{l1}. As angle β_1 is varied over its full 360° range, the end of phasor $\bar{V}_{dq1}$ moves along a circle with its centre located at the end of phasor $\bar{V}_{s1}$.

The rotation of phasor $\bar{V}_{dq1}$ with angle β_1 modulates both magnitude and the angle of phasor $\bar{V}_{xl1}$ and, therefore, both the transmitted real power, P_{1r}, and the reactive power, Q_{1r}, vary with β_1 in a sinusoidal manner [4 -5] . This process, of course, requires the voltage source representing SeV1 ($\bar{V}_{dq1}$) to supply and absorbs both reactive and real power, Q_{SeV1} and P_{SeV1}, which are also sinusoidal functions of angle β_1.

In order to establish the possible compensation range for the line 2, under the constraints imposed by the unrestricted compensation of line 1, it is helpful to decompose the overall compensating power provided for line 1 into reactive power Q_{SeV1} and real power P_{SeV1}. To this end, the injected voltage phasor $\bar{V}_{dq1}$ is decomposed into two components, one, V_{dq1q}, in quadrature and the other V_{dq1p}, in phase with the line current phasor $\bar{I}_1$. In particular, the in-phase component emulates a positive or negative resistance in series with the line impedance, while the quadrature component an inductive or capacitive reactance in series with the line impedance.

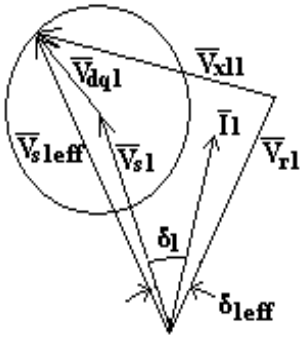

Fig. 3. Phasor diagram of System 1

The scalar product of V_{dq1q} and V_{dq1p} with $\bar{I}_1$ define Q_{SeV1} and P_{SeV1}, respectively. The component Q_{SeV1}, generated internally by SeV1, evidently provides series reactive compensation for line 1. The component P_{SeV1} provides real power compensation for line1, but this power must be supplied by SeV2 from line 2. It follows therefore that in order to satisfy the active power demand of SeV1, SeV2 must be operated so as the relationship P_{SeV2}=P_{SeV1}. Each of the SeV has been realized by a 24-pulse inverter configuration to reduce the presence of harmonic components in the inverter output voltage with quasi square wave operation.

In this paper, the two SeVs provide real and reactive series compensation for line 1 and line 2. The injected series voltages can be so chosen appropriately to force any desired current vector, respecting the thermal and stability limits, to flow on the line, hence establishing a corresponding power flow. Naturally, one SeV can inject a series voltage at any angle with respect to the line current, so to exchange also real power with the transmission line, only when the other SeV is also operating. In this case the exchanged real power at the terminals of the SeV with the line can flow to the terminals of the other SeV through the common DC-link. On the basis of power flow requests the SeV control adjusts the gating of the associated inverter to inject the related voltage vector in series with the transmission line.

The control structure of the IPFC is similar to that of the UPFC [2] with appropriate changes in the controlled variables and the necessary constraints imposed by the possible limitations of real power transfer. The IPFC control schemes used in this paper are shown in Fig. 4a-4b.

As shown in Fig. 4a, the operation of SeV1 is synchronized to line current $\tilde{i}_1$ and SeV2 to line current $\tilde{i}_2$ by two independent phase-locked loops. This enables each inverter to provide independent series reactive compensation and to keep operating under contingency conditions when the other line or inverter is out of service. The input to SeV1 ("prime" inverter) is either the desired real and reactive line power, P_{SeV1}^* and Q_{SeV1}^*, that are translated in the desired quadrature and phase component V_{dq1q}^* and V_{dq1p}^*, respectively. From these two components the desired magnitude and angle of the injected voltage phasor $\bar{V}_{dq1}$ are valued. The angle is added to the reference angle, while the magnitude $|\bar{V}_{dq1}|$ is compared to the actual value, derived from the measured injected voltage vectors $\tilde{v}_{dq1}$.

The control of SeV2 is different from that of SeV1 because it must support the operation of SeV1 by supplying the necessary real power from line 2 (see

Fig. 4b). This requirement means that, since the in-phase component of the injected compensating voltage is imposed on line 2 by the real power demand of line 1, the control of SeV2 can influence only the transmitted reactive power in its own line by controlling the quadrature component of the injected voltage $\tilde{v}_{dq2}$. Thus, the reference input to the control of SeV2 is the desired quadrature compensating voltage $V_{dq2q}{}^{*}$. This component is compared to the actual voltages component, V_{dq2q}, derived from the measured injected voltage vectors $\tilde{v}_{dq2}$. Then, the obtained error signal is the input signal for the SeV2 linear controller implemented to modify the angle γ_2 for SeV2.

In particular, the SeV linear controllers have been designed on the basis of the linearised model of the power system with IPFC installed (see Fig. 2).At this scope, considering in Fig. 2 the instantaneous voltages and currents values we have, for each single phase:

$$\begin{aligned} v_1 - v_{dq1} - v_{r1} &= L_{s1}\frac{di_1}{dt} + L_1\frac{di_1}{dt} \\ v_2 - v_{dq2} - v_{r2} &= L_{s2}\frac{di_2}{dt} + L_2\frac{di_2}{dt} \end{aligned} \quad (1)$$

Where the inverter output voltages are:

$$\begin{aligned} v_{dq1_a} &= k\cos(n\gamma_1)v_{dc}\sin(\omega t + \alpha_1 + \beta_1) \\ v_{dq1_b} &= k\cos(n\gamma_1)v_{dc}\sin(\omega t + \alpha_1 + \beta_1 - \frac{2}{3}\pi) \\ v_{dq1_c} &= k\cos(n\gamma_1)v_{dc}\sin(\omega t + \alpha_1 + \beta_1 - \frac{4}{3}\pi) \\ v_{dq2_a} &= k\cos(n\gamma_2)v_{dc}\sin(\omega t + \alpha_2 + \beta_2) \\ v_{dq2_b} &= k\cos(n\gamma_2)v_{dc}\sin(\omega t + \alpha_2 + \beta_2 - \frac{2}{3}\pi) \\ v_{dq2_c} &= k\cos(n\gamma_2)v_{dc}\sin(\omega t + \alpha_2 + \beta_2 - \frac{4}{3}\pi) \end{aligned} \quad (2)$$

In which α_1 and α_2 are the reference angles for line1 and line 2, respectively, β_1 and β_2 are the relative angle, respectively, of the two SeVs output voltage with respect to the line current. Moreover, for the power balance the following relation have to be satisfied:

$$P_{dc} = P_{SeV1} - P_{SeV2} \quad (3)$$

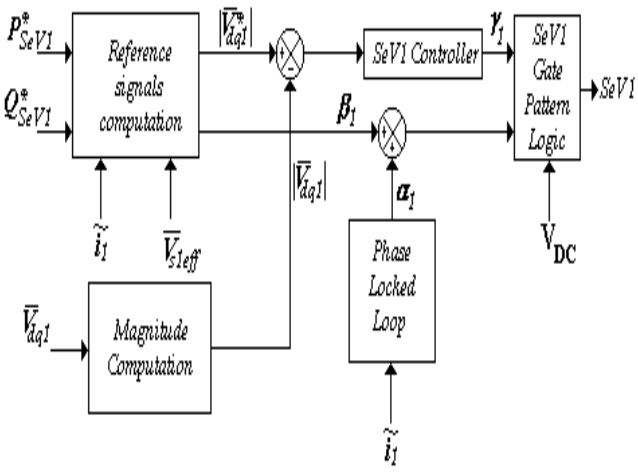

Fig. 4a. IPFC-SeV1 control scheme

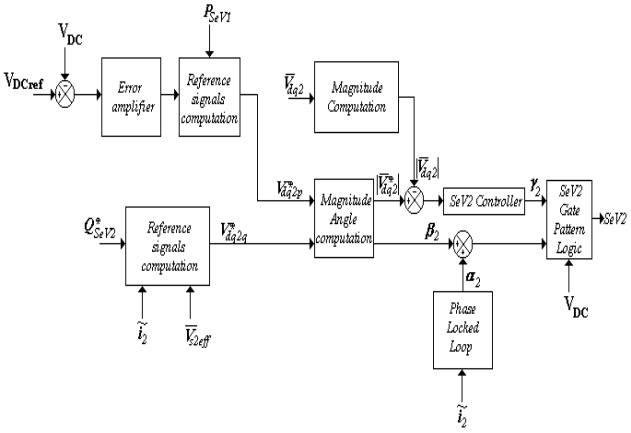

Fig. 4b. IPFC-SeV2 control scheme

Written the equations (2-4) in the d-q frame and linearised around a specific operating point, the IPFC can be represented by the following dynamic linear system:

$$\frac{d}{dt}\begin{bmatrix}\Delta i_{1d}\\ \Delta i_{1q}\\ \Delta i_{2d}\\ \Delta i_{2q}\\ \Delta v_{DC}\end{bmatrix} = \begin{bmatrix}k_{1a} & k_{2a} & 0 & 0 & k_{5a}\\ k_{1b} & k_{2b} & 0 & 0 & k_{5b}\\ 0 & 0 & k_{3c} & k_{4c} & k_{5c}\\ 0 & 0 & k_{3d} & k_{4d} & k_{5d}\\ k_{1e} & k_{2e} & k_{3e} & k_{4e} & 0\end{bmatrix}\begin{bmatrix}\Delta i_{1d}\\ \Delta i_{1q}\\ \Delta i_{2d}\\ \Delta i_{2q}\\ \Delta v_{DC}\end{bmatrix} + \begin{bmatrix}k_{6a} & 0\\ k_{6b} & 0\\ k_{6c} & 0\\ k_{6d} & 0\\ k_{6e} & k_{7e}\end{bmatrix}\begin{bmatrix}\gamma_1\\ \gamma_2\end{bmatrix} \quad (4)$$

Incompact-form:

$$\dot{x} = Ax + Bu \quad (5)$$

Where $x = \begin{bmatrix}\Delta i_{1d} & \Delta i_{1q} & \Delta i_{2d} & \Delta i_{2q} & \Delta v_{dc}\end{bmatrix}^T$,

$u = [\Delta\gamma_1 \quad \Delta\gamma_2]^T \in \Re^2$

In particular, in the paper the SeVs internal controller has been implemented to modify the angles γ_1 and γ_2.

3. Performance of IPFC System

Considering the model illustrated in section II the two IPFC control inputs are for the SeVs control scheme, the angles γ_1 and γ_2, respectively. As the SeVs are subject to the interacting operating limits of the IPFC through its DC-link, it is therefore desirable to co-ordinate the two control inputs to exploit their advantages and features to the maximum extent. For this aim the error signals from the reference injected voltage magnitude $\left|\bar{V}_{dq1}^{*}\right|$ and $\left|\bar{V}_{dq2}^{*}\right|$ for the two SeVs have been considered as further state variables.

The system (5) becomes:

$$\dot{\tilde{x}} = \tilde{A}\tilde{x} + \tilde{B}u$$
$$y = \tilde{C}\tilde{x} \qquad (6)$$

Where

$$\tilde{x} = \begin{bmatrix} x & y \end{bmatrix}^T \quad y = \begin{bmatrix} v_{dq1}^{\ err} & v_{dq2}^{\ err} \end{bmatrix}$$

$$\tilde{A} = \begin{vmatrix} A & 0 \\ C & 0 \end{vmatrix} \quad \tilde{B} = \begin{vmatrix} B \\ B1 \end{vmatrix} \quad B1 = \begin{vmatrix} k_{6f} & 0 \\ 0 & k_{7g} \end{vmatrix} \quad C = \begin{vmatrix} k_{8f} & k_{9f} & k_{10f} & 0 & 0 \\ 0 & 0 & k_{10g} & k_{11g} & k_{12g} \end{vmatrix}$$

The aim is to find the control law

$$u = K\tilde{x} = \begin{bmatrix} \gamma_1^{opt} & \gamma_2^{opt} \end{bmatrix}^T \qquad (7)$$

Which minimized the following index

$$J = \int_0^\infty y^T Q y + u^T R u \, dt \qquad (8)$$

Subject to the dynamic constraints expressed by (6).

$$K = R^{-1}\tilde{B}^T H \qquad (9)$$

Here the performance is to consider the DC-link voltage, that represents in both two cases a real measure of the actual operating condition and of the interactions between the inverters (SeV1 and SeV2) and to modify the control inputs γ_1 and γ_2, respectively. The simulation results of IPFC with different load compensation, power demand and control output are shown in Fig.5a.5b, 6a and 6b respectively.

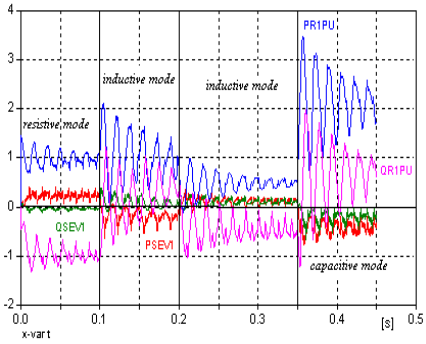

Fig. 5a. Waveforms showing the operation of the IPFC with SeV1 emulating resistive, inductive and capacitive compensation of line

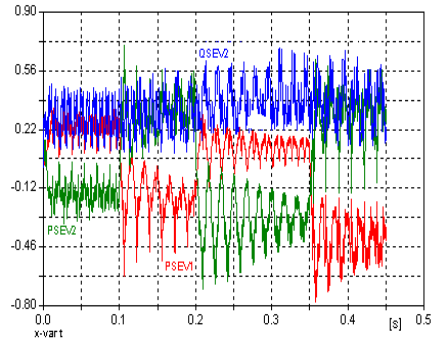

Fig 5b. Waveforms showing the operation of SeV2 providing the real power demand of SeV1 and inductive compensation for line 2.

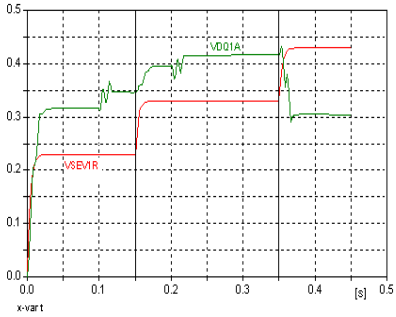

Fig.6a.SeV1. simulation results with Control-1

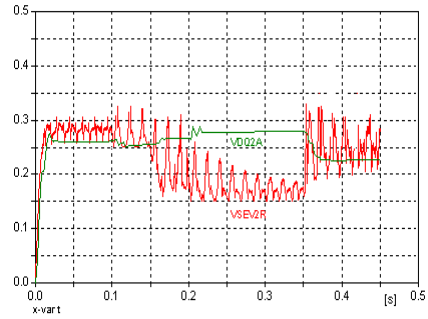

Fig.6b. SeV2 simulation results with Control-1

4. Simulation of IPFC in Power Flow

It is observed that when there is a difference in the angle between the two sending end voltages, transfer of real power from the line with higher angle to the line with lower angle occurs and thereby maintaining the stability. The output for a case where the first line has a phase angle of 45° and the second line has a phase angle of 0° is studied. It is observed that the real power at the load of line 2 is 520 KW as in Fig 8. The other cases of phase angle differences are also taken and the results are tabulated as in table 1.

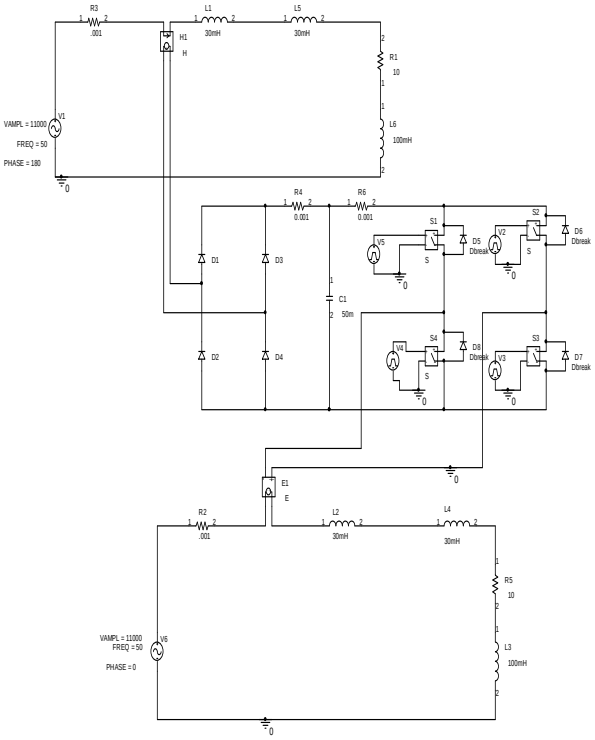

Fig. 7. Model of transmission line with phase difference

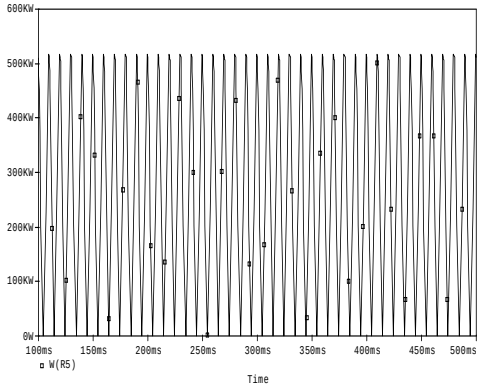

Fig. 8. Real Power at load end for system 1 with an angle of 45° and system 2 with an angle of 0°

S.No	Bus Angle at System 1	Bus Angle at System 2	Real power Measured at load of system 2
1.	180°	45°	450kW
2.	180°	90°	370kW
3.	270°	45°	880kW
4.	270°	90°	490kW
5.	270°	180°	25kW
6.	360°	45°	460kW
7.	360°	90°	425kW
8.	30°	20°	700kW
9.	30°	10°	750kW

Table . 1. Real power transferred for different angles

This circuit is also modeled and simulated. The outputs for the variations of the two sending end voltages are studied. The real power flows between higher angle to the lower angle, and the various values are tabulated.

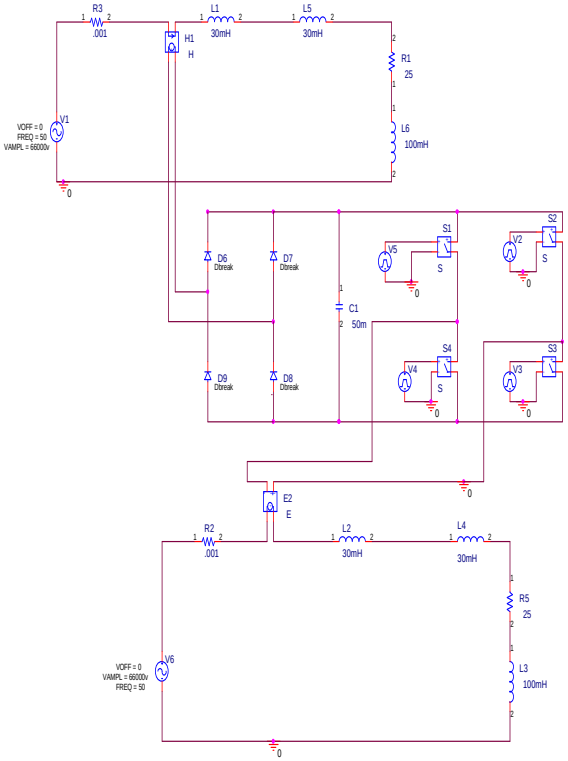

Fig. 9. Model of transmission line with voltage difference

The reactive powers at the individual line ends of 3 KV and 3.3 KV are taken .The output is as in Fig.10 and Fig 11.Then the reactive power is measured after including the Inter line power flow controller. It is observed that the reactive power flows from a line with high voltage to a line with low voltage. A case for which voltage of the first line is 3KV and the second line is 3.3KV is simulated and the resultant waveform is displayed in Fig 11.

S.NO	Voltage rating of Line 1(KV)	Reactive power at line 1	Voltage rating of Line 2(KV)	Reactive power at line 2	Transfer of reactive power
1	6.0	155 KVAR	6.6	188 KVAR	178 KVAR on 6KV line
2	10	430 KVAR	11	520 KVAR	495 KVAR on 10KV line
3	32	4.3 MVAR	33	5.2 MVAR	5.0 MVAR on 32KV line
4	64	17.5MVAR	66	21.2MVAR	21MVAR on 64KV line

Table . 2. Reactive power transferred for different voltages

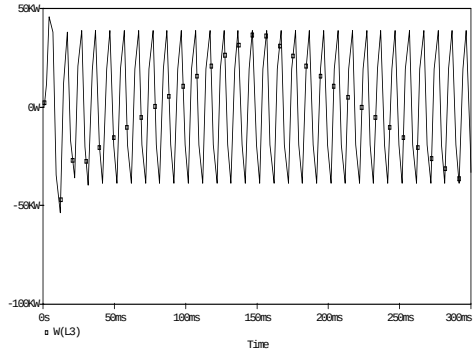

Fig. 10. The reactive power at the 3.0KV line is 39KVAR

The reactive power obtained through the IPFC from 3.3KV to 3.0KV line is measured to be 44KVAR on the 3.0 KV line. So it is concluded that the reactive power flows from a line with higher voltage to a line with lower voltage to maintain the balance. The different cases with various voltage combinations with their respective reactive power compensation are given in table 2.

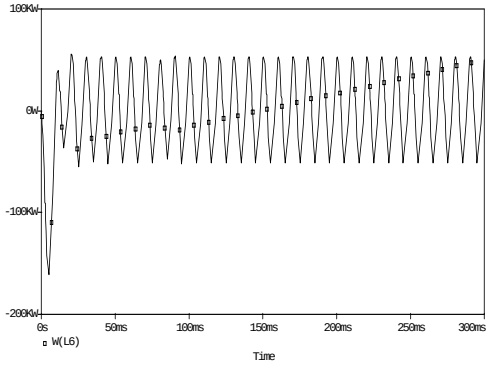

Fig 11.The reactive power at 3.3KV line is 52 KVAR

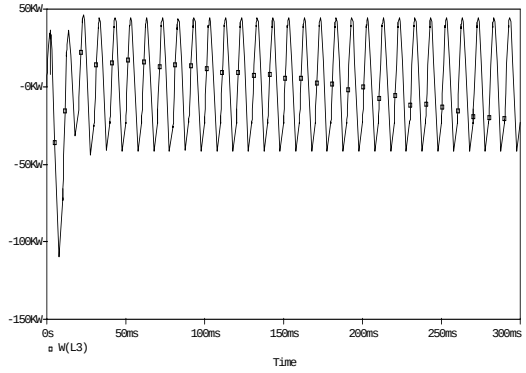

Fig. 12. The reactive power obtained through the IPFC from 3.3KV to 3.0KV line is 44KVAR on the 3.0 KV line

5. Conclusion

In this research, this controller has been demonstrated successfully in the IPFC system. Indeed, the main concept is to consider the DC-link voltage, that represents in both two cases a real measure of the actual operating condition and of the interactions between the inverters (SeV1 and SeV2) and to modify the control inputs. The simulation results show the improvement available by the proposed controller respect to the conventional one. The real power flows between higher angle to the lower angle, and the various values are clearly analyzed. So it is concluded that the reactive power flows from a line with higher voltage to a line with lower voltage to maintain the balance of a system.

References

1 Hingorani, N.G.*High power Electronics and Flexible AC Transmission System*, IEEE Power Eng. REV., July 1988.

2 B. M. Zhang, Q.F.Ding, *The development of FACTS and its control*, Proc. APSCOM-97, Hong Kong, November 1997, pp. 48-53.

3 M. H. Baker, R.J. Trow, *New FACTS controllers and how assess them*, Proceedings of APSCOM-97, Hong Kong, November 1997, pp.42-47.

4 N.G. Hingorani, L.Gyugi, *Understanding FACTS*", IEEE Press, 1999.

5 L.Gyugi, K.K. Sen, C. D. Schauder, *The Interline Power Flow Controller concept: a new approach to power flow management in transmission systems*, IEEE Trans. on Power Delivery, Vol.14, No. 3, July 1999, pp. 1115-1123.

6 S. Limyingcharoen, U. D. Annakkage, N. C. Pahalawaththa, *Fuzzy logic based unified power flow controllers for transient stability improvement*, IEE Proc.- Gener. Transm. Distrib., vol. 145, No. 3, May 1998, pp. 225-232.

7 H. W. Dommel, *Electro Magnetic Transient Program*, Refernce Manual (EMTP theory Book), August 1986.

8 Zhang X.P. *Modelling of the Inter line Power Flow controller and the generalized Unified Power Flow Controller (UPFC) in Newton power flow*, "IEE Proceedings on Generation Transmission-Distribution, Vol 150, No 3, PP 268-274, May 2003.